Eur. Phys. J. C 56, 279–285 (2008)
DOI 10.1140/epjc/s10052-008-0658-7

THE EUROPEAN PHYSICAL JOURNAL C

Regular Article – Theoretical Physics

Unparticle searches through gamma–gamma scattering

O. Çakır[1,a], K.O. Ozansoy[1,2,b]

[1] Department of Physics, Fakulty of Sciences, Ankara University, 06100 Tandogan, Ankara, Turkey
[2] Department of Physics, University of Wisconsin, Madison, WI 53706, USA

Received: 28 April 2008 / Revised version: 21 May 2008 /
Published online: 2 July 2008 –

Abstract. We investigate the effects of unparticles on $\gamma\gamma \to \gamma\gamma$ scattering for the photon collider mode of the future multi-TeV e^+e^- linear collider. We show the effects of unparticles on the differential, and total scattering cross sections for different polarization configurations. Considering 1-loop standard model background contributions from the charged fermions and $W^\pm$ bosons to the cross section, we calculate the upper limits on the unparticle couplings λ_0 to the photons for various values of the scaling dimension d $(1 < d < 2)$ at $\sqrt{s} = 0.5$–5 TeV.

1 Introduction

Recently, a mind-blowing, and very interesting, new physics proposal has been presented by Georgi [1]. According to this proposal, there could be a scale invariant sector with a nontrivial infrared fixed point living at a very high energy scale. Since any theory with massive fields cannot be scale invariant, the standard model (SM) is not a scale invariant theory. Therefore, such a scale invariant sector, if any, should consist of massless fields and would interact with the SM fields at the very high energies. One of the most striking low energy properties of that proposal is that using low energy effective theory considerations one can calculate the possible effects of such a scale invariant sector for TeV scale colliders.

In [1], the fields of a very high energy theory with a nontrivial fixed point are called Banks–Zaks (BZ) fields according to [2]. Interactions of BZ operators $\mathcal{O}_{\rm BZ}$ with the SM operators $\mathcal{O}_{\rm SM}$ are expressed by the exchange of particles with the very high energy mass scale $\mathcal{M}_{\mathcal{U}}^k$ in the following form:

$$\frac{1}{\mathcal{M}_{\mathcal{U}}^k} O_{\rm BZ} O_{\rm SM}\,, \tag{1}$$

where the BZ and SM operators are defined as $O_{\rm BZ} \in \mathcal{O}_{\rm BZ}$ with mass dimension $d_{\rm BZ}$, and $O_{\rm SM} \in \mathcal{O}_{\rm SM}$ with mass dimension $d_{\rm SM}$. The low energy effects of the scale invariant $\mathcal{O}_{\rm BZ}$ fields imply a dimensional transmutation. Thus, after dimensional transmutation, (1) is given by

$$\frac{C_{\mathcal{U}} \Lambda_{\mathcal{U}}^{d_{\rm BZ}-d}}{\mathcal{M}_{\mathcal{U}}^k} O_{\mathcal{U}} O_{\rm SM}\,, \tag{2}$$

where d is the scaling mass dimension of the unparticle operator $O_{\mathcal{U}}$ (in [1], $d = d_{\mathcal{U}}$), and the constant $C_{\mathcal{U}}$ is a coefficient function.

Using the low energy effective field theory approach, very briefly summarized above, in [1, 3] the main properties of the unparticle physics are presented. A list of Feynman rules for the unparticles coupled to the SM fields [4, 5], and several implications for collider phenomenology are given in [6–9]. In this paper, our calculations are based on the conventions of [4, 5].

Searching for new physics effects, the e^+e^- linear colliders have an exceptional advantage because of its appealing clean background and the options of $e\gamma$ and $\gamma\gamma$ colliders based on it. Recently, for new physics searches, as a multi-TeV energy electron–positron linear collider, the compact linear collider (CLIC) proposed and developed at CERN, is seriously taken into account. Numerous works on the CLIC have been done so far [10–14]. As other e^+e^- linear colliders, the CLIC would have e^-e^-, $e\gamma$ and $\gamma\gamma$ collider options and the possibilities of polarized e^+ and e^- beams. In this paper, we consider the $\gamma\gamma$ collider option of the CLIC to search for unparticle physics effects. Our results can easily be extended for other possible future multi-TeV scale linear electron–positron colliders [15]. In [16, 17], a detailed analysis of the $\gamma\gamma$ option of an e^+e^- collider has been given. Since the $\gamma\gamma \to \gamma\gamma$ process can only occur at loop level in SM, it gives a good opportunity to test for new physics which has tree level contributions to the scattering amplitude [18–20]. Regarding this process, as new physics searches, for example, supersymmetry [19, 20], large extra dimensions [21, 22], and noncommutative space-time effects [23] have been taken into account. Here, we study the effects of the unparticles on this process.

2 $\gamma\gamma$ scattering

The lowest order SM contributions to the $\gamma\gamma \to \gamma\gamma$ process are 1-loop contributions of the charged fermions and

[a] email: ocakir@science.ankara.edu.tr
[b] email: oozansoy@physics.wisc.edu

$W^{\pm}$ bosons. In the limits of the Mandelstam parameters obeying $s, |t|, |u| \gg M_W^2$, and using certain symmetry arguments given in [18–20], those 1-loop contributions can be expressed briefly. We present the corresponding 1-loop SM amplitudes in Appendix A.1. The analysis of Fox et al. [24] highlights that the existence of the scalar unparticle operator leads to conformal symmetry breaking when the Higgs operator gets a vacuum expectation value. If this symmetry breaking occurs at low energies, some strong constraints are imposed on the unparticle sector. Here, we assume that the effects of the unparticle sector at future high energy collider energies could be measurable.

Using the low energy effective field theory assumptions of [3–5], the photon–photon–scalar unparticle interaction can be parametrized as $\lambda_0 F_{\mu\nu} F^{\mu\nu} O_{\mathcal{U}} / \Lambda_U^d$, where λ_0 is an effective coupling of order $\mathcal{O}(1)$ and $F_{\mu\nu}$ is the photon field strength. We use the appropriate form of the scalar unparticle propagator, $\Delta_F(q^2) = \frac{A_d}{2\sin(d\pi)}(-q^2)^{d-2}$. Since the Mandelstam parameter $s > 0$, there is a complex phase factor due to the s channel amplitude. Thus, for an s channel propagator one can consider $(-s^2)^{d-2} = (s)^{d-2} \mathrm{e}^{-\mathrm{i}d\pi}$ [4, 5]. The implications of such a complex factor could be studied only through interference terms.[1] The interesting features of this phase through s channel interference between SM and unparticle amplitudes have been discussed by [3]. Here, we present a more detailed study of the effects of unparticles on the differential and total cross sections for different initial polarization configurations to cover a wide range of the parameter space of the unparticle sector.

There are three tree level diagrams contributing to $\gamma(p_1)\gamma(p_2) \to \gamma(p_3)\gamma(p_4)$ scattering amplitude from the exchange of the scalar unparticle U_{S} which can be expressed with the following amplitudes:

$$M^s_{\mathcal{U}_{\mathrm{S}}} = \left[\epsilon^{\mu}(p_1)\left[4\mathrm{i}\frac{\lambda_0}{\Lambda_U^d}[-p_1.p_2 g_{\mu\nu} + p_{1\nu}p_{2\mu}]\right]\epsilon^{\nu}(p_2)\right] \times \left[\epsilon^{\rho *}(p_3)\left[4\mathrm{i}\frac{\lambda_0}{\Lambda_U^d}[-p_3.p_4 g_{\rho\sigma} + p_{3\sigma}p_{4\rho}]\right]\epsilon^{\sigma *}(p_4)\right] \times \left[\frac{\mathrm{i}A_d}{2\sin d\pi}\left[-(p_1+p_2)^2\right]^{d-2}\right], \quad (3)$$

$$M^t_{\mathcal{U}_{\mathrm{S}}} = \left[\epsilon^{\rho *}(p_3)\left[4i\frac{\lambda_0}{\Lambda_U^d}[p_1.p_3 g_{\mu\rho} - p_{1\rho}p_{3\mu}]\right]\epsilon^{\mu}(p_1)\right] \times \left[\epsilon^{\sigma *}(p_4)\left[4\mathrm{i}\frac{\lambda_0}{\Lambda_U^d}[p_2.p_4 g_{\nu\sigma} - p_{2\sigma}p_{4\nu}]\right]\epsilon^{\nu}(p_2)\right] \times \left[\frac{\mathrm{i}A_d}{2\sin d\pi}\left[-(p_1-p_3)^2\right]^{d-2}\right], \quad (4)$$

$$M^u_{\mathcal{U}_{\mathrm{S}}} = \left[\epsilon^{\sigma *}(p_4)\left[4\mathrm{i}\frac{\lambda_0}{\Lambda_U^d}[p_1.p_4 g_{\mu\sigma} - p_{1\sigma}p_{4\mu}]\right]\epsilon^{\mu}(p_1)\right] \times \left[\epsilon^{\rho *}(p_3)\left[4\mathrm{i}\frac{\lambda_0}{\Lambda_U^d}[p_2.p_3 g_{\nu\rho} - p_{2\rho}p_{3\nu}]\right]\epsilon^{\nu}(p_2)\right]$$

$$\times \left[\frac{\mathrm{i}A_d}{2\sin d\pi}[-(p_1-p_4)^2]^{d-2}\right], \quad (5)$$

with

$$A_d = \frac{16\pi^{5/2}}{(2\pi)^{2d}} \frac{\Gamma(d+1/2)}{\Gamma(d-1)\Gamma(2d)}, \quad (6)$$

where Λ_U is the energy scale for the scalar unparticle operator.[2] In the calculations of the unpolarized and polarized cross sections, we use the expressions given in the appendix. To give an idea of unparticle effects on the unpolarized differential cross section, $\mathrm{d}\sigma/\mathrm{d}\cos\theta$ with and without unparticle effects is plotted in Fig. 1. In this figure, we choose $\lambda_0/\Lambda_{\mathcal{U}} = 0.2\ \mathrm{TeV}^{-1}$ and the values $d = 1.1$, 1.3 and 1.5 at $\sqrt{s_{ee}} = 1$ TeV. One can see from Fig. 1, that the unparticle effect increases while the scaling dimension d approaches to 1. The unpolarized total cross section with respect to the center of mass energy of the mono-energetic photon beams with and without unparticle contributions is plotted in Fig. 2. For the unparticle effects in that plot, we assume that $\lambda_0/\Lambda_{\mathcal{U}} = 0.1\ \mathrm{TeV}^{-1}$, and we compare the shape of the distribution for $d = 1.1$ and 1.5.

For the polarized cross section calculations of the backscattered photons, we define M_{ijkl} to be the helicity am-

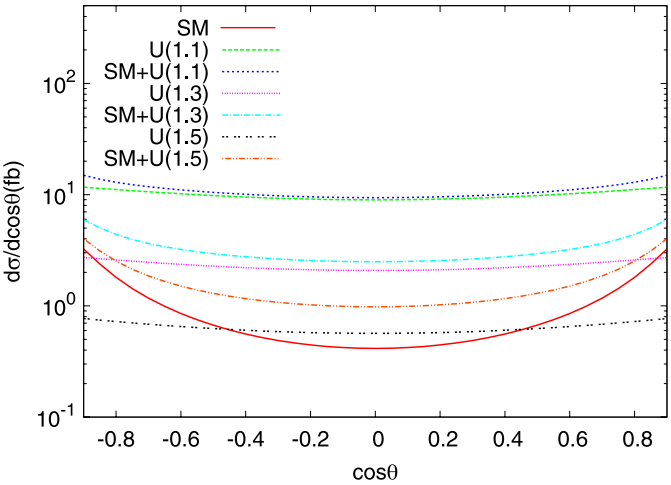

Fig. 1. The unpolarized differential cross sections with pure SM and with SM+$\mathcal{U}$ effects at $\sqrt{s_{ee}} = 1$ TeV. For the unparticle effects, $\lambda_0/\Lambda_{\mathcal{U}} = 0.2\ \mathrm{TeV}^{-1}$, $d = 1.1$, 1.3 and 1.5

[1] After we put the first version of the present paper online, Chang et al. [8], have discussed the implications of this phase in the same context as our paper does.

[2] Very recently, after the first version of this paper appeared online, Grinstein et al. [25] have commented on several issues related to the unparticle literature. Besides the comments on the scaling dimensions and the corrections in the form of the propagator for vector and tensor unparticles, they have pointed out that a generic unparticle scenario generates contact interactions between particles. Therefore, there could be generically a contribution like, for example, our (5), but without a q-dependent propagator. In our analysis we have not considered such contributions, in other words, for very high energy physics effects due to the unparticle sector, we consider only $O_{\mathrm{SM}}O_U$ type interactions between unparticles and SM particles, and we do not consider $O_{\mathrm{SM}}O_{\mathrm{SM}}$ type contact interactions between SM fields.

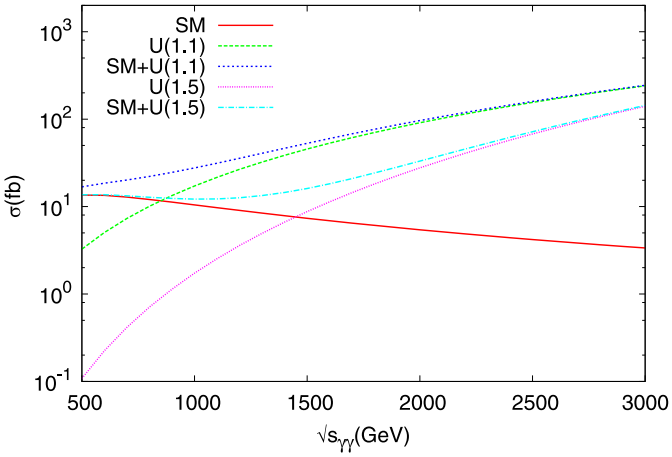

Fig. 2. The unpolarized cross sections for SM and SM+$\mathcal{U}$. For unparticle effects, $\lambda_0/\Lambda_{\mathcal{U}} = 0.1$ TeV^{-1}, $d = 1.1$ and 1.5

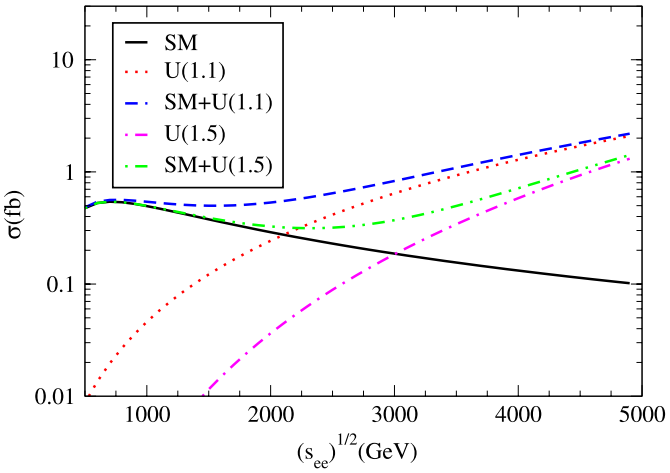

Fig. 3. The total polarized cross sections for SM and for SM+$\mathcal{U}$ with the polarization configuration (++). Here, we assume $\lambda_0/\Lambda_U = 0.1$ TeV^{-1}, $d = 1.1$ and 1.5

plitude of $\gamma\gamma \to \gamma\gamma$ scattering. We use the following definitions:

$$|M(++)|^2 = \sum_{i,j} |M(++ij)|^2 \,, \tag{7}$$

$$|M(+-)|^2 = \sum_{i,j} |M(+-ij)|^2 \,, \tag{8}$$

where the summations are over the helicities of the outgoing photons. Therefore, depending on the initial fermion polarization P_e, and the laser beam polarization h_l, the differential scattering cross section in terms of the average helicity h_γ can be written as

$$\frac{\mathrm{d}\sigma}{\mathrm{d}\cos\theta} = \frac{1}{(64\pi)} \int_{x_{1\,\min}}^{0.83} \mathrm{d}x_1 \int_{x_{2\,\min}}^{0.83} \mathrm{d}x_2 \frac{f(x_1) f(x_2)}{\hat{s}} \times \left[\left(\frac{1 + h_\gamma(x_1) h_\gamma(x_2)}{2} \right) \left| M^{\mathrm{SM}+\mathcal{U}_\mathrm{S}}(++) \right|^2 + \left(\frac{1 - h_\gamma(x_1) h_\gamma(x_2)}{2} \right) \left| M^{\mathrm{SM}+\mathcal{U}_\mathrm{S}}(+-) \right|^2 \right] , \tag{9}$$

where $f(x)$ is the photon number density and h_γ is the average helicity function presented in Appendix A.3, and, as $\sqrt{s_{ee}} \equiv \sqrt{s}$ is the center of mass energy of the e^+e^- collider, $\sqrt{\hat{s}} = \sqrt{x_1 x_2 s_{ee}}$ is the reduced center of mass energy of the back-scattered photon beams. Furthermore, $x = E_\gamma/E_e$ is the energy fraction taken by the back-scattered photon beam. In our analysis, we follow the usual collider assumptions (see, for example, [22, 23]) and we take $|h_l| = 1$ and $|P_e| = 0.9$. Considering the kinematical region $M_W^2/s, |M_W^2/t|, |M_W^2/u| < 1$ the dominant amplitudes for the SM 1-loop contributions are given in Appendix A.1. In our analysis, we use the cuts $\pi/6 < \theta < 5\pi/6$ and $\sqrt{0.4} < x_i < x_{\max}$, which have been used in the literature, where $x_{\max}$ is the maximum energy fraction of the back-scattered photon, and its optimum value is 0.83.

In Figs. 3 and 4, to present a schematic behavior of the polarized cross section with or without unparticle contributions; we plot the total cross section for two different polarization configurations of the initial beams. We use the following definitions for the polarization configurations: $(++) \equiv (++++) = (P_{e1} = 0.9, h_{l1} = 1; P_{e2} = 0.9, h_{l2} = 1)$, and $(+-) \equiv (+-+-) = (P_{e1} = 0.9, h_{l1} = -1; P_{e2} = 0.9, h_{l2} = -1)$. Those figures could give an idea of the dependence on the scaling dimension d of the unparticle contribution.

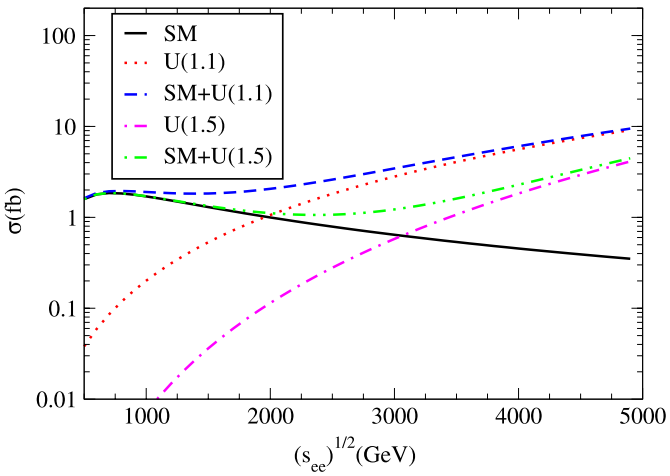

Fig. 4. The total polarized cross sections for SM and for SM+$\mathcal{U}$ with the polarization configuration (+−). Here, we assume that $\lambda_0/\Lambda_U = 0.1$ TeV^{-1}, $d = 1.1$ and 1.5

3 Limits

Searching for unparticle effects in high energy $\gamma\gamma \to \gamma\gamma$ scattering, we extract the upper limits on the unparticle coupling λ_0 regarding the 95% C.L. analysis. In the calculations, we use the standard chi-square analysis for the

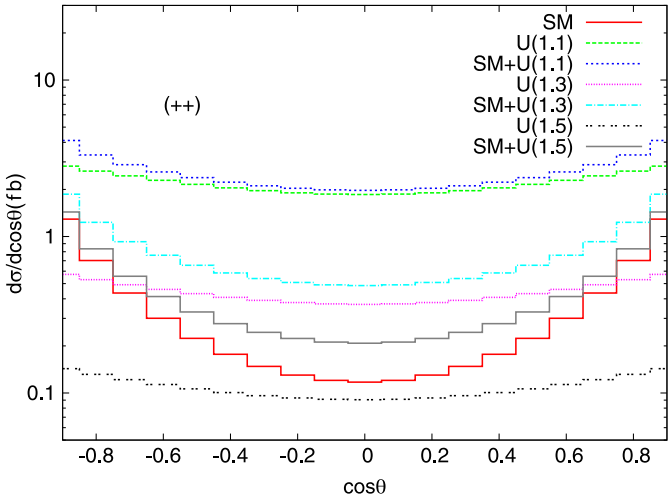

Fig. 5. The angular distribution for SM and for SM+$\mathcal{U}$ cross sections with the polarization configuration (++). Here, we assume that $\lambda_0/\Lambda_U = 0.3\ \mathrm{TeV}^{-1}$, $d = 1.1$ and 1.3 at $\sqrt{s_{ee}} = 1$ TeV

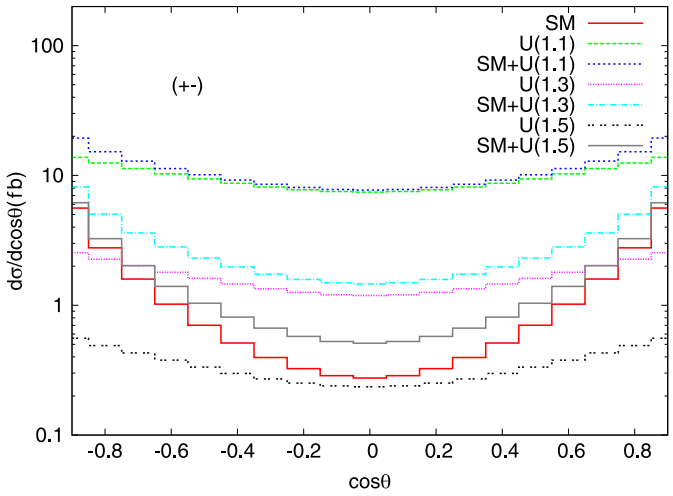

Fig. 6. The angular distribution for SM and for SM+$\mathcal{U}$ cross sections with the polarization configuration (+−). Here, we assume that $\lambda_0/\Lambda_U = 0.3\ \mathrm{TeV}^{-1}$, $d = 1.1$ and 1.3 at $\sqrt{s_{ee}} = 1$ TeV

following χ^2 function:

$$\chi^2 = \sum_i \left[\frac{\frac{\mathrm{d}\sigma_i}{\mathrm{d}\cos\theta}(\mathrm{SM}) - \frac{\mathrm{d}\sigma_i}{\mathrm{d}\cos\theta}(\mathrm{SM}+\mathcal{U})}{\delta\frac{\mathrm{d}\sigma_i}{\mathrm{d}\cos\theta}(\mathrm{SM})} \right]^2 , \quad (10)$$

where $\delta\frac{\mathrm{d}\sigma}{\mathrm{d}\cos\theta}$ is the error of the measurement. For a one sided chi-square analysis, we assume $\chi^2 \geq 2.7$, and we take the two possible luminosity values, $\mathcal{L} = 100\,\mathrm{fb}^{-1}$ and $\mathcal{L} = 1000\,\mathrm{fb}^{-1}$ per year. We calculate the upper limits on the coupling of the scalar unparticles by performing a fit to a binned photon angular distribution as shown in Figs. 5 and 6. For the signal and background calculation, we take into account only the statistical error on the SM distribution. However, systematic errors should be considered including e^+/e^- beam conversion, photon–photon collisions and detector effects for the detection of photons, and if they are controlled well, the limits can be improved and benefit from the advantage of high luminosity. Our limits

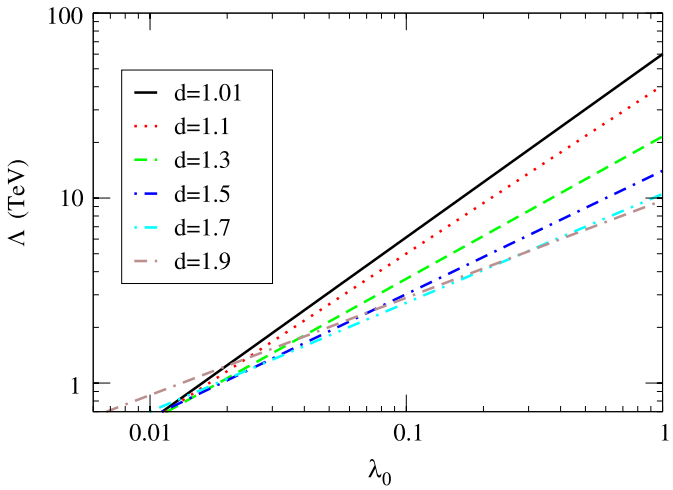

Fig. 7. Upper limits on the scalar unparticle coupling λ_0 depending on $\Lambda_\mathcal{U}$ for (++) polarization at CLIC, with 5 TeV energy

Table 1. Upper limits on the λ_0 for the polarization configuration (++) for $\mathcal{L} = 100(1000)\ \mathrm{fb}^{-1}$ and $\Lambda_U = 1000$ GeV

$\sqrt{s}$ (GeV)	$d = 1.01$	$d = 1.1$	$d = 1.3$	$d = 1.5$	$d = 1.7$	$d = 1.9$
500	0.0865(0.065)	0.113(0.085)	0.194(0.1455)	0.316(0.237)	0.479(0.359)	0.551(0.413)
1000	0.0605(0.0455)	0.0745(0.056)	0.1115(0.0835)	0.1585(0.1185)	0.2095(0.157)	0.2105(0.1575)
3000	0.0300(0.0225)	0.0335(0.0250)	0.0403(0.030)	0.0458(0.0345)	0.0485(0.0365)	0.0393(0.0295)
5000	0.0213(0.016)	0.0225(0.017)	0.0245(0.0185)	0.0253(0.019)	0.0243(0.0183)	0.0178(0.0133)

Table 2. Upper limits on the λ_0 for the polarization configuration (+−) for $\mathcal{L} = 100(1000)\ \mathrm{fb}^{-1}$ and $\Lambda_U = 1000$ GeV

$\sqrt{s}$ (GeV)	$d = 1.01$	$d = 1.1$	$d = 1.3$	$d = 1.5$	$d = 1.7$	$d = 1.9$
500	0.069(0.052)	0.091(0.0685)	0.1625(0.122)	0.2765(0.2075)	0.432(0.324)	0.504(0.378)
1000	0.0478(0.0358)	0.0593(0.0443)	0.0925(0.0695)	0.1375(0.1033)	0.1875(0.1408)	0.1915(0.1435)
3000	0.0235(0.0178)	0.0265(0.0198)	0.0333(0.0250)	0.0398(0.0298)	0.0435(0.0328)	0.0358(0.0268)
5000	0.0165(0.0125)	0.018(0.0135)	0.0205(0.0153)	0.022(0.0165)	0.0218(0.0163)	0.0165(0.0123)

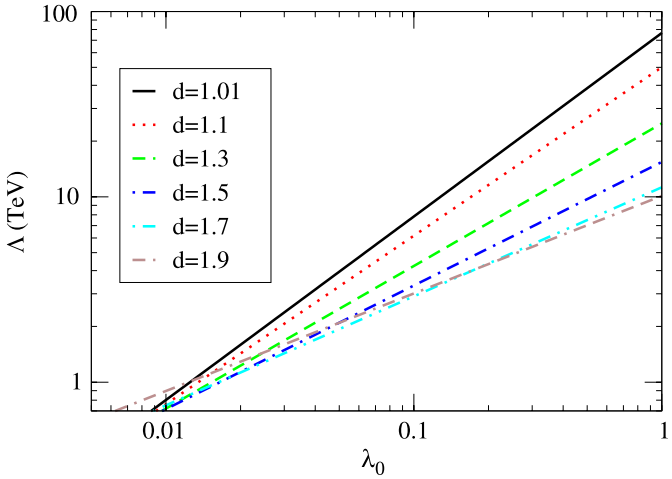

Fig. 8. Upper limits on the scalar unparticle coupling λ_0 depending on $\Lambda_{\mathcal{U}}$ for $(+-)$ polarization at CLIC, with 5 TeV energy

on λ_0 are presented in Tables 1 and 2 for two polarization configurations.

Since the cross section is proportional to $\lambda_0^4/\Lambda_{\mathcal{U}}^{4d}$, our limits can be restated regarding the corresponding behaviors of λ_0 and $\Lambda_{\mathcal{U}}$. In Figs. 7 and 8, for the polarization configuration $(++)$ and $(+-)$, we plot the corresponding behaviors of Λ_U and λ_0. The right hand side of each curve is ruled out according to the 95% C.L. analysis. For the analysis schemes discussed above similar results can easily be obtained for the other center of mass energies with low/high luminosities.

4 Conclusion

For different values of the scaling dimension d, we put upper limits on λ_0 assuming that scalar unparticle effects on the polarized cross section can be distinguished from the SM contribution at 95% C.L. In our analysis, we consider the multi-TeV CLIC electron–positron collider, which will be launched at the CERN, for center of mass energies $\sqrt{s} = 0.5$–$5.0\,\text{TeV}$ and luminosities $\mathcal{L} = 100\,\text{fb}^{-1}$ and $\mathcal{L} = 1000\,\text{fb}^{-1}$ per year. Our limits are consistent with the limits calculated from other low and high energy physics implications [6, 7]. Our calculations show that the limits on λ_0 get more stringent as one increases the luminosity and the center of mass energy of the collider.

Acknowledgements. It is a pleasure to thank B. Balantekin for many helpful conversations and discussions. K.O.O. would like to thank the members of the Nuclear Theory Group of the University of Wisconsin for their hospitality, and acknowledges the support through the Scientific and Technical Research Council (TUBITAK) BIDEP-2219 Grant. The work of O.C. was supported in part by the State Planning Organization (DPT) under Grant No. DPT-2006K-120470 and in part by the Turkish Atomic Energy Authority (TAEA) under Grant No. VII-B.04.DPT.1.05.

A Appendix

A.1 1-loop SM amplitudes

The lowest order SM contributions to the $\gamma\gamma \to \gamma\gamma$ process are 1-loop contributions of the charged fermions and $W^{\pm}$ bosons. There are 16 helicity amplitudes contributing at the 1-loop level, and only three of them can be stated independently. We can choose them $(++++)$, $(+++-)$, and $(++--)$. In the limits $s, |t|, |u| \gg M_W^2$, the only significant contributions come from the $(++++)$ polarization configuration, and that can be expressed in the following form [18–20]. For the W boson contribution, we have

$$\begin{aligned}
&\frac{M^{(W)}_{++++}(\hat{s},\hat{t},\hat{u})}{\alpha^2} \\
&\approx 12 + 12\left(\frac{\hat{u}-\hat{t}}{\hat{s}}\right)\left[\ln\left(\frac{-\hat{u}-\mathrm{i}\epsilon}{m_W^2}\right) - \ln\left(\frac{-\hat{t}-\mathrm{i}\epsilon}{m_W^2}\right)\right] \\
&\quad + 16\left(1-\frac{3\hat{t}\hat{u}}{4\hat{s}^2}\right)\left\{\left[\ln\left(\frac{-\hat{u}-\mathrm{i}\epsilon}{m_W^2}\right) - \ln\left(\frac{-\hat{t}-\mathrm{i}\epsilon}{m_W^2}\right)\right]^2 + \pi^2\right\} \\
&\quad + 16\hat{s}^2\left[\frac{1}{\hat{s}\hat{t}}\ln\left(\frac{-\hat{s}-\mathrm{i}\epsilon}{m_W^2}\right)\ln\left(\frac{-\hat{t}-\mathrm{i}\epsilon}{m_W^2}\right)\right. \qquad \text{(A.1)} \\
&\quad \left. + \frac{1}{\hat{s}\hat{u}}\ln\left(\frac{-\hat{s}-\mathrm{i}\epsilon}{m_W^2}\right)\ln\left(\frac{-\hat{u}-\mathrm{i}\epsilon}{m_W^2}\right)\right] \\
&\quad + \frac{16\hat{s}^2}{\hat{t}\hat{u}}\ln\left(\frac{-\hat{t}-\mathrm{i}\epsilon}{m_W^2}\right)\ln\left(\frac{-\hat{u}-\mathrm{i}\epsilon}{m_W^2}\right), \qquad \text{(A.2)}
\end{aligned}$$

for the fermion loop,

$$\begin{aligned}
&\frac{M^{(f)}_{++++}(\hat{s},\hat{t},\hat{u})}{\alpha^2 Q_f^4} \\
&\approx -8 - 8\left(\frac{\hat{u}-\hat{t}}{\hat{s}}\right)\left[\ln\left(\frac{-\hat{u}-\mathrm{i}\epsilon}{m_f^2}\right) - \ln\left(\frac{-\hat{t}-\mathrm{i}\epsilon}{m_f^2}\right)\right] \\
&\quad - 4\left(\frac{\hat{t}^2+u^2}{s^2}\right)\left\{\left[\ln\left(\frac{-\hat{u}-\mathrm{i}\epsilon}{m_f^2}\right) - \ln\left(\frac{-\hat{t}-\mathrm{i}\epsilon}{m_f^2}\right)\right]^2 + \pi^2\right\},
\end{aligned} \qquad \text{(A.3)}$$

where Q_f is the fermion charge, m_f is the mass of the fermion, and for the helicity amplitudes we use $M_{h_1h_2h_3h_4}$ with the photon helicities $h_i = \pm$. Using the assumptions given in [19, 20], the other significant helicity amplitudes can be generated by using the relations $M_{+-+-}(\hat{s},\hat{t},\hat{u}) = M_{++++}(\hat{u},\hat{t},\hat{s})$ and $M_{+--+}(\hat{s},\hat{t},\hat{u}) = M_{+-+-}(\hat{s},\hat{u},\hat{t})$.

A.2 Expressions for unparticle contributions

In the calculations, we assume the following center of mass reference frame kinematical relations:

$$\begin{aligned}
&p_1^\mu = E(1,0,0,1)\,, \quad p_2^\mu = E(1,0,0,-1)\,, \\
&p_3^\mu = E(1,\sin\theta,0,\cos\theta)\,, \\
&p_4^\mu = E(1,-\sin\theta,0,-\cos\theta)\,, \\
&\epsilon_1^\mu = -\frac{1}{\sqrt{2}}(0,h_1,\mathrm{i},0)\,, \quad \epsilon_2^\mu = \frac{1}{\sqrt{2}}(0,-h_2,\mathrm{i},0)\,,
\end{aligned} \qquad \text{(A.4)}$$

where $\epsilon_1 \equiv \epsilon_1(h_1), \epsilon_2 \equiv \epsilon_1(h_2)$, etc., $h_1, h_2 = \{+,-\}$ stand for the polarizations, and we assume that the summation is over the final state polarizations.

Therefore, one may find the following terms:

$$\begin{aligned}
\left|M^s_{\mathcal{U}_S}(++)\right|^2 &= \left|M^s_{\mathcal{U}_S}(--)\right|^2 = \frac{1}{8}[f(d)]^2[s]^{2d} \\
\left|M^s_{\mathcal{U}_S}(+-)\right|^2 &= \left|M^s_{\mathcal{U}_S}(-+)\right|^2 = 0 \\
\left|M^t_{\mathcal{U}_S}(++)\right|^2 &= \left|M^t_{\mathcal{U}_S}(+-)\right|^2 = \left|M^t_{\mathcal{U}_S}(-+)\right|^2 \\
&= \left|M^t_{\mathcal{U}_S}(--)\right|^2 = \frac{1}{16}[f(d)]^2[-t]^{2d} \\
\left|M^u_{\mathcal{U}_S}(++)\right|^2 &= \left|M^u_{\mathcal{U}_S}(+-)\right|^2 = \left|M^u_{\mathcal{U}_S}(-+)\right|^2 \\
&= \left|M^u_{\mathcal{U}_S}(--)\right|^2 = \frac{1}{16}[f(d)]^2[-u]^{2d}\,.
\end{aligned} \tag{A.5}$$

The phase $\exp(-\mathrm{i}d\pi)$ is associated with the $s-t$ and $s-u$ channel interference:

$$\begin{aligned}
2\,\mathrm{Re}\left(M^{s*}_{\mathcal{U}_S}M^t_{\mathcal{U}_S}\right)(++) &= 2\,\mathrm{Re}\left(M^{s*}_{\mathcal{U}_S}M^t_{\mathcal{U}_S}\right)(--) \\
&= \frac{1}{8}[f(d)]^2[s]^d[-t]^d\cos(d\pi)\,, \\
2\,\mathrm{Re}\left(M^{s*}_{\mathcal{U}_S}M^t_{\mathcal{U}_S}\right)(+-) &= 2\,\mathrm{Re}\left(M^{s*}_{\mathcal{U}_S}M^t_{\mathcal{U}_S}\right)(-+) = 0\,, \\
2\,\mathrm{Re}\left(M^{s*}_{\mathcal{U}_S}M^u_{\mathcal{U}_S}\right)(++) &= 2\,\mathrm{Re}\left(M^{s*}_{\mathcal{U}_S}M^u_{\mathcal{U}_S}\right)(--) \\
&= \frac{1}{8}[f(d)]^2[s]^d[-u]^d\cos(d\pi)\,, \\
2\,\mathrm{Re}\left(M^{s*}_{\mathcal{U}_S}M^u_{\mathcal{U}_S}\right)(+-) &= 2\,\mathrm{Re}\left(M^{s*}_{\mathcal{U}_S}M^u_{\mathcal{U}_S}\right)(-+) = 0\,, \\
2\,\mathrm{Re}\left(M^{t*}_{\mathcal{U}_S}M^u_{\mathcal{U}_S}\right)(+-) &= 2\,\mathrm{Re}\left(M^{t*}_{\mathcal{U}_S}M^u_{\mathcal{U}_S}\right)(-+) = 0\,, \\
2\,\mathrm{Re}\left(M^{t*}_{\mathcal{U}_S}M^u_{\mathcal{U}_S}\right)(++) &= 2\,\mathrm{Re}\left(M^{t*}_{\mathcal{U}_S}M^u_{\mathcal{U}_S}\right)(--) \\
&= \frac{1}{8}[f(d)]^2[tu]^d\,,
\end{aligned} \tag{A.6}$$

where

$$f(d) = \frac{8\lambda_0^2 A_d}{\Lambda^{2d}\sin(d\pi)}\,. \tag{A.7}$$

After the first version of this paper appeared online, similar work has been appeared [8, 9]. Our revised equations including the unparticle phase are in agreement with those papers. If one takes the average over the squared helicity amplitudes, then one gets

$$\begin{aligned}
|\bar{M}|^2 = \frac{1}{4}[f(d)]^2 \big\{&[s]^{2d} + [-t]^{2d} + [-u]^{2d} + [tu]^d \\
&+ \left([s]^d[-t]^d + [s]^d[-u]^d\right)\cos(d\pi)\big\}\,.
\end{aligned} \tag{A.8}$$

A.3 Polarization functions

Let h_e and h_l be the polarizations of the electron beam and the laser photon beam, respectively. According to [16, 17], the following function can be defined:

$$\begin{aligned}
C(x) = &\frac{1}{1-x} + 1 - x - 4r(1-r) \\
&- h_\mathrm{e}h_\mathrm{l}rz(2r-1)(2-x)\,,
\end{aligned} \tag{A.9}$$

where $r = \frac{x}{z(1-x)}$, and $z = 4E_eE_\mathrm{l}/m_e^2$ describes the laser photon energy. Therefore, the photon number density is given by

$$f(x, h_\mathrm{e}, h_\mathrm{l}, z) = \left(\frac{2\pi\alpha^2}{m_e^2 z\sigma_c}\right)C(x)\,, \tag{A.10}$$

where

$$\begin{aligned}
\sigma_c = &\left(\frac{2\pi\alpha^2}{m_e^2 z}\right)\left[\left(1 - \frac{4}{z} - \frac{8}{z^2}\right)\ln(z+1) + \frac{1}{2} + \frac{8}{z} + \frac{1}{2(z+1)^2}\right] \\
&+ h_\mathrm{e}h_\mathrm{l}\left(\frac{2\pi\alpha^2}{m_e^2 z}\right)\left[\left(1 + \frac{2}{z}\right)\ln(z+1)\right. \\
&\left. - \frac{5}{2} + \frac{1}{z+1} - \frac{1}{2(z+1)^2}\right]\,.
\end{aligned} \tag{A.11}$$

The average helicity is given by

$$\begin{aligned}
h_\gamma(x, h_\mathrm{e}, h_\mathrm{l}, z) = \frac{1}{C(x)}\Bigg\{&h_\mathrm{e}\left[\frac{x}{1-x} + x(2r-1)^2\right] \\
&- h_\mathrm{l}(2r-1)\left(1 - x + \frac{1}{1-x}\right)\Bigg\}\,.
\end{aligned} \tag{A.12}$$

References

1. H. Georgi, Phys. Rev. Lett. **98**, 221 601 (2007) [hep-ph/0703260]
2. T. Banks, A. Zaks, Nucl. Phys. B **196**, 189 (1982)
3. H. Georgi, Phys. Lett. B **650**, 275 (2007) [arXiv:0704.2457 [hep-ph]]
4. K. Cheung, W.Y. Keung, T.C. Yuan, Phys. Rev. Lett. **99**, 051 803 (2007) [arXiv:0704.2588 [hep-ph]]
5. K. Cheung, Phys. Rev. D **76**, 055 003 (2007) [arXiv:0706.3155 [hep-ph]]
6. L. Anchordoqui, H. Goldberg, arXiv:0709.0678 [hep-ph]
7. A.B. Balantekin, K.O. Ozansoy, Phys. Rev. D **76**, 095 014 (2007) [arXiv:0710.0028 [hep-ph]]
8. C.F. Chang, K. Cheung, T.C. Yuan, arXiv:0801.2843 [hep-ph]
9. T. Kikuchi, N. Okada, M. Takeuchi, arXiv:0801.0018 [hep-ph]
10. CLIC Physics Working Group, E. Accomando et al., hep-ph/0412251
11. ECFA/DESY LC Physics Working Group, J.A. Aguilar-Saavedra et al., hep-ph/0106315
12. R.W. Assmann et al., A 3-TeV e^+e^- linear collider based on CLIC technology, CERN-2000-008, Geneva, 2000
13. R.W. Assmann et al., CLIC contribution to the technical review committee on a 500 GeV e^+e^- linear collider, CERN-2003-007, Geneva, 2003
14. A. De Roeck, hep-ph/0311138
15. S. Dawson, M. Oreglia, Ann. Rev. Nucl. Part. Sci. **54**, 269 (2004) [hep-ph/0403015]
16. I.F. Ginzburg, G.L. Kotkin, V.G. Serbo, V.I. Telnov, Nucl. Instrum. Methods **205**, 47 (1983)
17. I.F. Ginzburg, G.L. Kotkin, S.L. Panfil, V.G. Serbo, V.I. Telnov, Nucl. Instrum. Methods A **219**, 5 (1984)

18. G. Jikia, A. Tkabladze, Phys. Lett. B **323**, 453 (1994) [hep-ph/9312228]
19. G.J. Gounaris, P.I. Porfyriadis, F.M. Renard, Eur. Phys. J. C **9**, 673 (1999) [hep-ph/9902230]
20. G.J. Gounaris, P.I. Porfyriadis, F.M. Renard, Phys. Lett. B **452**, 76 (1999)
21. K. M. Cheung, Phys. Rev. D **61**, 015 005 (2000) [hep-ph/9904266]
22. H. Davoudiasl, Phys. Rev. D **60**, 084 022 (1999) [hep-ph/9904425]
23. J.L. Hewett, F.J. Petriello, T.G. Rizzo, Phys. Rev. D **64**, 075 012 (2001) [hep-ph/0010354]
24. P.J. Fox, A. Rajaraman, Y. Shirman, Phys. Rev. D **76**, 075 004 (2007) [arXiv:0705.3092 [hep-ph]]
25. B. Grinstein, K. Intriligator, I.Z. Rothstein, arXiv:0801.1140 [hep-ph]